STAT3 upregulation in pituitary somatotroph adenomas induces growth hormone hypersecretion

Cuiqi Zhou,[1,2] Yonghui Jiao,[2,3] Renzhi Wang,[2,3] Song-Guang Ren,[1] Kolja Wawrowsky,[1] and Shlomo Melmed[1]

[1]Department of Medicine, Cedars-Sinai Medical Center, Los Angeles, California, USA. [2]Joint Pituitary Research Center of Cedars-Sinai Medical Center and Peking Union Medical College Hospital and [3]Department of Neurosurgery, Peking Union Medical College Hospital, Chinese Academy of Medical Sciences, Peking Union Medical College, Beijing, China.

Pituitary somatotroph adenomas result in dysregulated growth hormone (GH) hypersecretion and acromegaly; however, regulatory mechanisms that promote GH hypersecretion remain elusive. Here, we provide evidence that STAT3 directly induces somatotroph tumor cell GH. Evaluation of pituitary tumors revealed that STAT3 expression was enhanced in human GH-secreting adenomas compared with that in nonsecreting pituitary tumors. Moreover, STAT3 and GH expression were concordant in a somatotroph adenoma tissue array. Promoter and expression analysis in a GH-secreting rat cell line (GH3) revealed that STAT3 specifically binds the *Gh* promoter and induces transcription. Stable expression of STAT3 in GH3 cells induced expression of endogenous GH, and expression of a constitutively active STAT3 further enhanced GH production. Conversely, expression of dominant-negative STAT3 abrogated GH expression. In primary human somatotroph adenoma-derived cell cultures, STAT3 suppression with the specific inhibitor S3I-201 attenuated *GH* transcription and reduced GH secretion in the majority of derivative cultures. In addition, S3I-201 attenuated somatotroph tumor growth and GH secretion in a rat xenograft model. GH induced STAT3 phosphorylation and nuclear translocation, indicating a positive feedback loop between STAT3 and GH in somatotroph tumor cells. Together, these results indicate that adenoma GH hypersecretion is the result of STAT3-dependent GH induction, which in turn promotes STAT3 expression, and suggest STAT3 as a potential therapeutic target for pituitary somatotroph adenomas.

Introduction

Pituitary tumors are benign monoclonal adenomas that account for approximately 15% of intracranial tumors (1). They arise from highly differentiated anterior pituitary cells expressing one or more pituitary hormone gene products. Pituitary somatotroph adenomas (growth hormone–secreting [GH-secreting] pituitary adenomas) are associated with dysregulated GH hypersecretion, leading to acromegaly, a disorder of disproportionate skeletal, tissue, and organ growth (2).

Enhanced understanding of mechanisms underlying somatotroph adenoma pathogenesis is required for elucidation of novel cell targets because of limitations of current therapies, which include surgery, radiotherapy, somatostatin receptor ligands, and a GHR antagonist (2–4). These approaches are challenged by unique side effects, moderate patient-specific efficacy, and inability to directly target persistent postoperative GH hypersecretion in aggressive or recurrent tumors (2, 3). Multiple neurotransmitter pathways as well as a variety of peripheral feedback signals regulate GH secretion (5, 6). Transcription factors paired-like homeodomain factor 1 (*PROP1*) and POU class 1 homeobox 1 (*POU1F1*) determine somatotroph development and proliferation, and commitment to synthesizing and secreting GH (2, 7), but are not dysregulated in somatotroph tumorigenesis. Aberrant growth factor signaling as well as cell-cycle–regulating genes contribute to the pathogenesis of somatotroph adenomas (2, 8), yet proximal regulatory mechanisms enabling GH hypersecretion in these adenomas remain elusive.

STAT3, a member of the STAT family, participates in cellular responses to cytokines and growth factors (9). Phosphorylated cytoplasmic STAT3 dimerizes and translocates to the nucleus, subsequently regulating target genes to modulate cell proliferation, survival and differentiation (10–12), and overexpression and/or constitutive activation of STAT3 are encountered in human cancers (11, 13). STAT3 is a cancer therapeutic target, as constitutive STAT3 inhibition by small-molecule inhibitors is associated with cell growth suppression and cell death (14–16), and phase I/II oncology trials using STAT3 inhibition are ongoing (17). In the pituitary, STAT3 mediates gp130-controlled corticotroph cell proliferation and function (18, 19), and STAT3 acts as a critical regulator for leukemia inhibitory factor–mediated proopiomelanocortin expression and adrenocorticotrophin secretion (19–23).

In this study, we provide evidence that STAT3 directly induces GH in somatotroph tumor cells. Increased STAT3 expression observed in human somatotroph adenoma tissues is concordant with GH expression, and STAT3 specifically bound the rat *Gh* promoter and activated *Gh* transcription. STAT3-induced GH expression was further enhanced by constitutively activated STAT3 (STAT3-C) and abrogated by dominant-negative STAT3 (STAT3-DN). Pharmacologic suppression of STAT3 decreased GH and also attenuated xenografted somatotroph tumor growth in vivo. Attenuating STAT3 signaling dose-dependently suppressed GH in primary cell cultures derived from human somatotroph adenomas. Moreover, we show that GH induces STAT3 phosphorylation and nuclear translocation, indicating the presence of mutual

Conflict of interest: The authors have declared that no conflict of interest exists.
Submitted: July 23, 2014; **Accepted:** January 29, 2015.
Reference information: *J Clin Invest*. 2015;125(4):1692–1702. doi:10.1172/JCI78173.

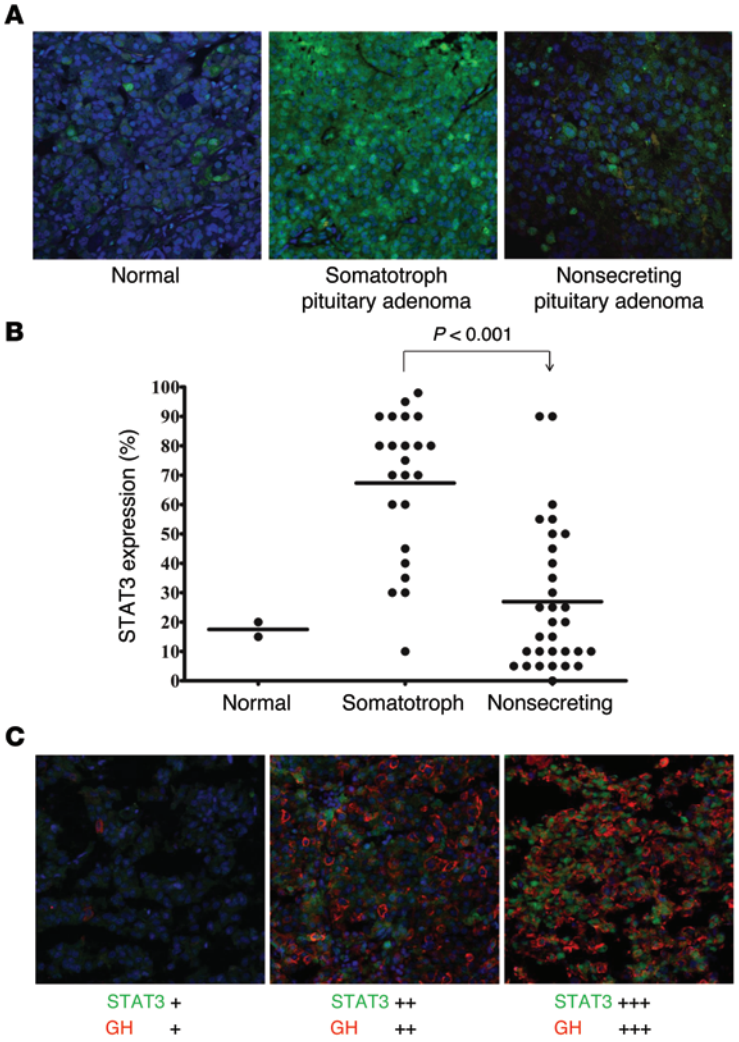

Figure 1. STAT3 expression in human pituitary tumor specimens, as assessed by confocal immunofluorescence. (**A**) Abundant STAT3 expression in somatotroph adenomas, with weak STAT3 staining in normal pituitary tissues and low STAT3 staining in a nonsecreting adenoma. Green signal, STAT3 staining; blue signal, DAPI nuclear staining; yellow signal, autofluorescence background. Original magnification, ×63. (**B**) Quantification of STAT3 expression. STAT3 expression was evaluated as a percentage of positively stained cells in 2 normal pituitary tissues, 23 somatotroph adenomas, and 31 nonsecreting adenomas. horizontal bars indicate the median. Unpaired *t* test, $P < 0.001$. (**C**) Representative images of concordant expression of STAT3 and GH in 35 somatotroph adenomas. Left, middle, and right panels depict discrete, moderate, and abundant staining of STAT3 and GH, respectively. Green signal, STAT3 staining; red signal, GH staining; blue signal, DAPI nuclear staining. Original magnification, ×63.

intrapituitary feedback regulation of STAT3 and GH. These results elucidate a mechanism that we believe to be novel underlying GH hypersecretion in pituitary somatotroph adenomas, whereby abundantly expressed adenoma STAT3 induces GH. The results provide a rationale for STAT3 as a potential therapeutic target to abrogate somatotroph tumor growth and dysregulated GH hypersecretion.

Results

STAT3 is abundantly expressed in human somatotroph adenomas and correlates with GH. As the STAT3 expression profile is unknown in human pituitary tumors, we assessed STAT3 expression by confocal immunofluorescence in 23 pituitary somatotroph adenomas, 31 nonsecreting pituitary tumors, and 2 normal tissue specimens. Expression was semiquantified as a percentage of positively stained cells. Weak STAT3 expression (18%) was detected in 2 normal pituitary tissue specimens, while low-to-moderate STAT3 staining (27% ± 4%) was observed in 31 nonsecreting pituitary tumors. STAT3 expression was significantly enhanced in somatotroph adenomas (67% ± 5%) as compared with nonsecreting pituitary tumor expression (unpaired *t* test, $P < 0.001$) (Figure 1, A and B).

We further costained STAT3 and GH by confocal immunofluorescence in a tissue array derived from 35 pituitary somatotroph adenomas and counted GH- or STAT3-positive cells separately. STAT3 and GH expression levels correlated significantly (Pearson χ^2 test, $P < 0.05$). Nine somatotroph adenomas with discrete GH signals exhibited weak STAT3 immunoreactivity (Figure 1C), and seven specimens showed moderate GH staining with moderate-to-high levels of STAT3 expression (Figure 1C). In 4 somatotroph adenomas exhibiting abundant GH expression, strong STAT3 immunoreactive signals were detected in up to 90% of tumor cells (Figure 1C).

STAT3 binds the rat Gh promoter and actives Gh transcription. Since no human somatotroph cell lines are available, we used rat GH3 cells (secreting both GH and prolactin) to study mechanisms for STAT3 actions in vitro. We screened the rat *Gh* promoter with Genomatix MatInspector and detected several potential STAT-binding sites (Figure 2A), indicating that *Gh* may act as a direct STAT3 target gene. Similar STAT-binding motifs are also located on the human *GH* promoter. Accordingly, we performed ChIP to identify STAT3 binding to the rat *Gh* promoter. GH3 cells were fixed and sonicated into 200- to 800-bp chromatin DNA fragments. Equal amounts of chromatin DNA were incubated with IgG-negative control or STAT3 antibody, respectively. Chromatin DNA captured by protein G beads was used as a template, and 3 pairs of promoter primers were designed for PCR. Primer 1 is the furthest from the transcriptional initiation site and primer 3 is the closest. As shown in Figure 2B, anti-STAT3–immunoprecipitated DNA with the enriched STAT locus was strongly amplified by primer pair 3, indicating specific STAT3 binding to the *Gh* promoter around this region.

To further measure *Gh* promoter activity in response to STAT3, we constructed two different rat *Gh* promoter plasmids, –4,192/+167 and –1,752/+167, in $pGL_{4.10}$ vector and created stable STAT3 transfectants to perform dual luciferase reporter assays. We transfected GH3 cells with pIRES2-ZsGreen1 controls or STAT3/pIRES2-ZsGreen1 plasmids and selected stable transfectants expressing ZsGreen. Equal numbers of STAT3/pIRES2-ZsGreen1 and pIRES2-ZsGreen1 stable transfectants were seeded in 24-well plates (5×10^5 cells per well) and transfected with the rat *Gh* promoter –4,192/+167, –1,752/+167, or $pGL_{4.10}$ vector as control, respectively. As shown in Figure 2C, STAT3 overexpression resulted in approximately 2-fold induction of *Gh* promoter activity compared with pIRES2-ZsGreen1, using both –4,192/+167 and –1,752/+167 promoters.

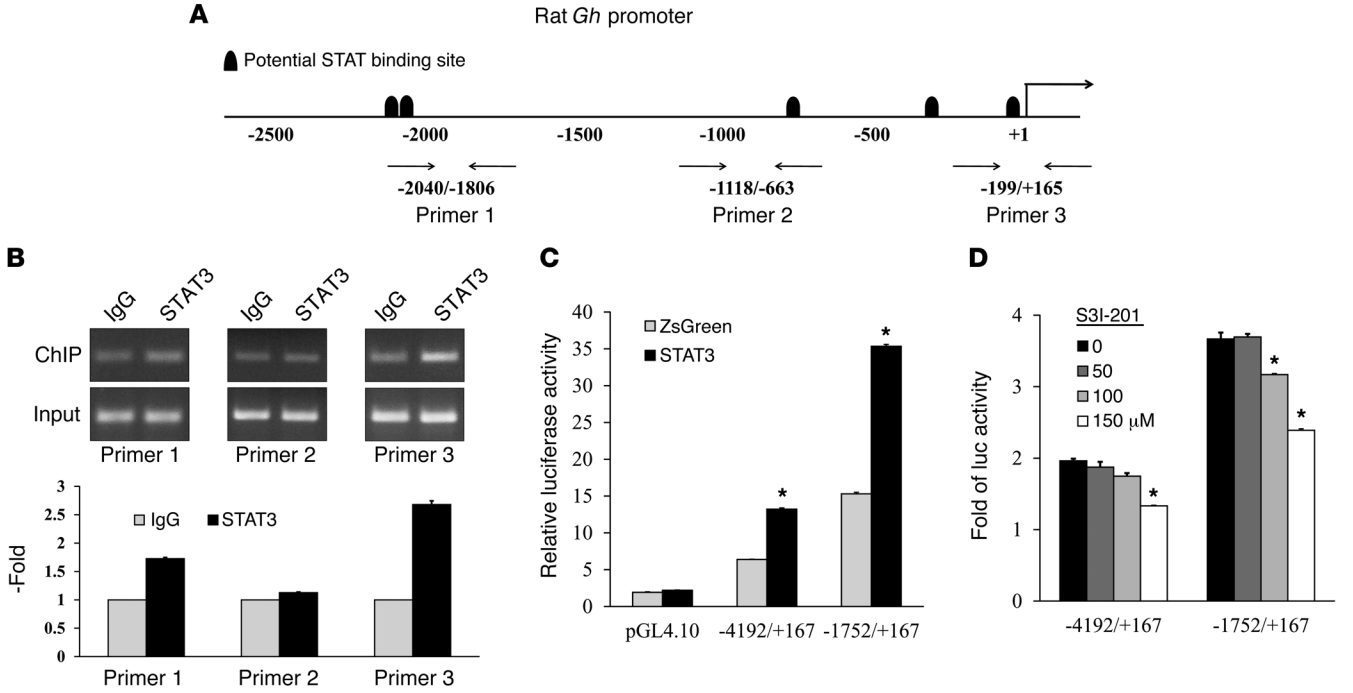

Figure 2. STAT3 binds the rat *Gh* promoter and activates *Gh* transcription. (**A**) Representation of potential STAT-binding motifs on the rat *Gh* promoter and 3 primer pairs designed for ChIP. (**B**) STAT3 binds the *Gh* promoter, as assessed by ChIP. Normalized inputs of GH3 chromatin DNA were pulled down by STAT3 or negative IgG antibodies. The DNA template was amplified by PCR using primer pairs 1–3. Quantitative ChIP results are shown. Ratios of the "ChIP band" to the "input band" were calculated, and IgG controls were normalized to 1. ChIP experiments and PCR reactions were repeated twice, and quantification is presented as mean ± SEM. (**C**) STAT3 activates *Gh* transcription, as assessed by a dual-luciferase reporter assay. Equal amounts of STAT3 or pIRES2-ZsGreen1 (ZsGreen) stable cells (5×10^5 cells per well) were transfected with the rat *Gh* promoter –4,192/+167, –1,752/+167, or pGL4.10 control, and luciferase activity was measured. (**D**) STAT3 inhibitor S3I-201 suppresses *Gh* transcription. GH3 cells were transfected with rat *Gh* promoter –4,192/+167, –1,752/+167, or pGL4.10 control and treated with increasing amounts of S3I-201. Transcriptional activities of rat *Gh* promoter –4,192/+167 and –1,752/+167 were both normalized to pGL4.10 controls. Ten ng pGL4.74 (hRluc/TK) plasmid was cotransfected to normalize transfection efficiency. Experiments were repeated 3 times. **C** and **D** show representative experiments, and cells were transfected or treated in triplicate wells. Results are presented as mean ± SEM. Student's *t* test, $^*P < 0.01$.

In addition, we used a specific STAT3 inhibitor, S3I-201, to attenuate endogenous STAT3 expression (24, 25) and measured *Gh* promoter activity. S3I-201 targets the Src homology 2 dimerization domain of STAT3 and inhibits STAT3 dimerization, DNA binding, and target gene activation (24). We transfected GH3 cells with rat *Gh* promoters (–4,192/+167 or –1,752/+167), treated them with increasing amounts of S3I-201 (50–150 μM), and measured luciferase activity. As shown in Figure 2D, the STAT3 inhibitor S3I-201 suppressed transcriptional activity of both *Gh* promoters by up to 35% at 150 μM.

STAT3 overexpression induces GH expression and secretion. As STAT3 binds and activates the *Gh* promoter, we assessed STAT3 regulation of endogenous GH expression in GH3 stable transfectants. We transfected pIRES2-ZsGreen1, wild-type STAT3, STAT3-C, and STAT3-DN plasmids in GH3 cells, respectively, and selected stable transfectants. Stable cells expressing ZsGreen were sorted prior to performing experiments to ensure expression. *Gh* mRNA expression was measured by real-time PCR using *Gapdh* as internal control. As shown in Figure 3A, overexpressed STAT3 increased *Gh* mRNA 1.7-fold and was further enhanced by STAT3-C (2.5-fold), while STAT3-DN with the Y705F mutation did not show *Gh* induction compared with controls. In contrast to *Gh* expression, prolactin (*Prl*) mRNA levels were lower in stable STAT3-C transfectants but were not altered in STAT3 and STAT3-DN stable transfectants, indicating specificity of the *Gh* induction. Cell lysates analyzed by Western blotting verified that GH protein abundance was altered similarly to mRNA levels (Figure 3B), i.e., upregulated STAT3 induced GH, which was further enhanced by STAT3-C. Furthermore, STAT3-DN abolished STAT3-induced GH protein expression. In contrast, prolactin was attenuated by STAT3-C and was not modified by STAT3-DN. Furthermore, we transiently infected GH3 cells with STAT3-DN in a lentiviral vector. Similar to STAT3-DN stable transfection, lenti-STAT3-DN transfection resulted in attenuated GH expression in GH3 cells as compared with lentiviral controls. We also infected GH3 cells with lenti-*Stat3* shRNA, and silencing endogenous STAT3 resulted in suppressed GH expression (Supplemental Figure 1; supplemental material available online with this article; doi:10.1172/JCI78173DS1). In addition to GH expression, STAT3-C also increased GH secretion. After stable GH3 transfectants were serum starved for 48 hours, media GH concentrations in STAT3-C stable cells were increased by 50%, while prolactin levels decreased by 50% (Figure 3C).

STAT3 inhibitor S3I-201 attenuates both GH expression and secretion. As STAT3 abundance increases GH expression, we used the STAT3 inhibitor S3I-201 to impair endogenous STAT3 expression and examine GH production. We serum starved GH3 cells for 24 hours, treated them with increasing amounts of

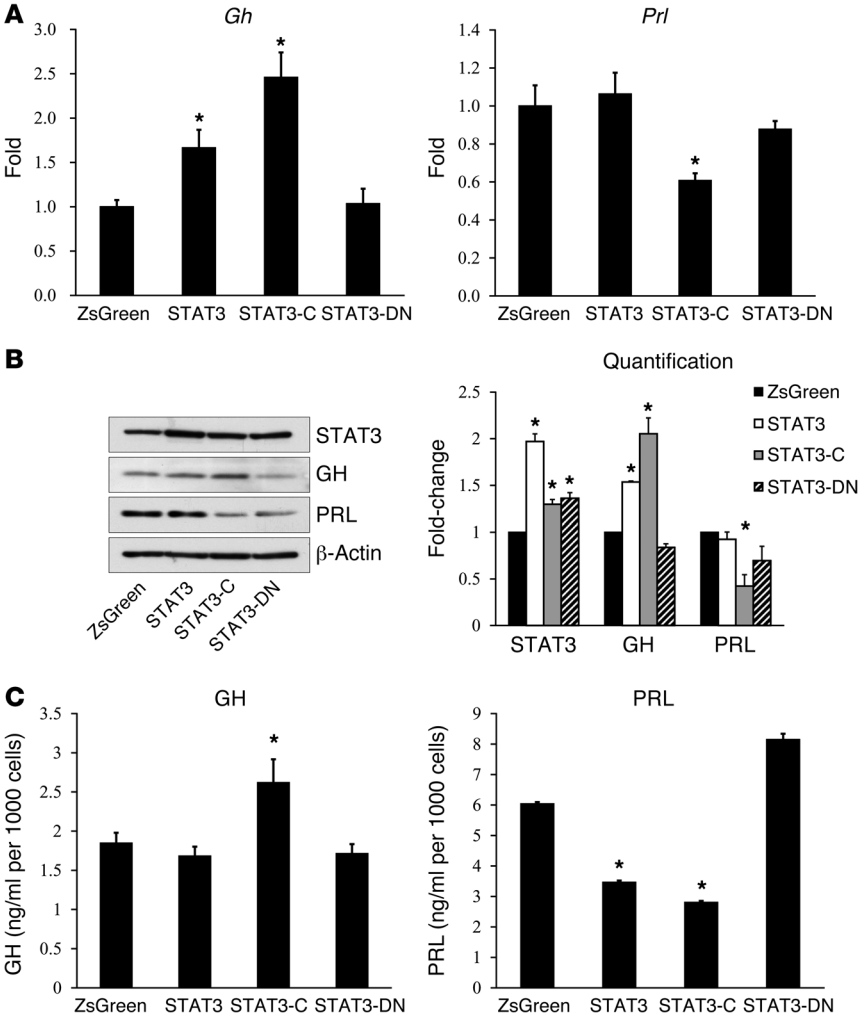

Figure 3. STAT3 induces GH expression and secretion. GH3 cells were transfected with pIRES2-ZsGreen1, STAT3, STAT3-C, or STAT3-DN and selected for stable transfectants. STAT3 increased (**A**) *Gh* mRNA and (**B**) protein expression, (**A**) as measured by real-time PCR or (**B**) Western blotting, and also induced GH secretion, (**C**) as assessed by RIA. Prolactin was measured to verify specific GH responses to STAT3. Real-time PCR and Western blotting were repeated twice. RIA was repeated twice and performed in 4 wells per represented value. **A** and **C** show representative experiments. Results are presented as mean ± SEM. Student's *t* test, $^*P < 0.05$.

S3I-201 (50–125 μM), and harvested cell lysates after 5 minutes and 20 hours, respectively. We also collected cell culture media to measure GH and PRL levels. As assessed by Western blotting, S3I-201 dose-dependently attenuated STAT3 phosphorylation at Tyr705 within 5 minutes, and decreased GH and total STAT3 protein were also observed at 20 hours (Figure 4A). Prolactin expression was not altered appreciably. We repeated experiments in GC and GH3 cells cultured with serum and obtained similar results; i.e., GH expression was dose-dependently suppressed by S3I-201 (data not shown). STAT3 Tyr705 phosphorylation was specifically decreased by S3I-201, while phosphorylation and expression of STAT1 and STAT5 were not attenuated in either GH3 or GC cells (Supplemental Figure 2). Similar to protein expression, GH secretion in the culture media was dose-dependently attenuated by S3I-201, whereas prolactin secretion exhibited an opposite trend (Figure 4B), further supporting the specificity of STAT3 action on GH.

GH promotes STAT3 phosphorylation and nuclear translocation. As GH-dependent tyrosyl phosphorylation of STAT1, STAT3, STAT5A, and STAT5B occurs in fibroblast, liver, and melanoma cells (26–28), we examined GH effects on somatotroph cell STAT3. We first used Western blotting to confirm GH receptor (GHR) expression in GH3 and GC cells, using HCT116 colon cells as positive controls. As shown in Figure 5A, both HCT116 and GC cells expressed the GHR (~70 kDa); GH3 cells expressed a weak band at approximately 70 kDa and a stronger band at approximately 100 kDa. Next, we treated GH3 cells with increasing amounts of GH (0–500 ng/ml) for 10 minutes and observed dose-dependent STAT3 Tyr705 phosphorylation, while total STAT3 expression was not changed, as measured by Western blot (Figure 5B). We further assessed STAT3 nuclear translocation in response to GH by transfecting GC cells with STAT3/pEGFP-N3 plasmids, which express a fusion STAT3-GFP protein, because GH3 cells are loosely adherent with floating clusters and difficult to image. STAT3/pEGFP-N3 and pEGFP-N3 control transfectants were serum starved overnight and separately treated with GH (500 ng/ml) or vehicle for 6 hours. Accumulation of nuclear STAT3-GFP was observed in GH-treated cells by fluorescent microscopy (Figure 5C). These results show that both STAT3 phosphorylation and activation are induced by GH in somatotroph cells.

STAT3 inhibitor S3I-201 attenuates GH3 cell growth in vitro and xenografted somatotroph tumor growth in vivo. As STAT3 may regulate cell proliferation, we examined S3I-201 effects on somatotroph tumor cell growth in vitro. We treated GH3 cells with increasing amounts of S3I-201 and measured cell proliferation by using WST-1 cell proliferation reagent and BrdU incorporation. Compared with vehicle-treated controls, S3I-201–treated GH3 cells exhibited up to 56% reduction of WST-1 absorbance after 72 hours. BrdU staining of S3I-201–treated GH3 cells was reduced up to 52% compared with that of control cells after 48 hours, similar to results obtained with the WST-1 assay (Figure 6A). Similar results were also obtained in GC cells (data not shown).

Based on these findings, we next evaluated S3I-201 effects on somatotroph tumor xenografts generated by injecting GH3 cells in the left lumbar area of 4-week-old female Wistar Furth rats ($n = 30$). After 1 week, once the tumor size reached approximately 100 mm^3, S3I-201 or vehicle alone was then injected intravenously at 5 mg/kg every 2 or 3 days for 2 weeks. Each group comprised 15 rats, and tumors were measured every 2 to 3 days after S3I-201 injection. Compared with vehicle-treated control tumors ($n = 15$), which continued to grow, S3I-201 treatment of somatotroph tumor xenografts ($n = 15$) significantly attenuated tumor

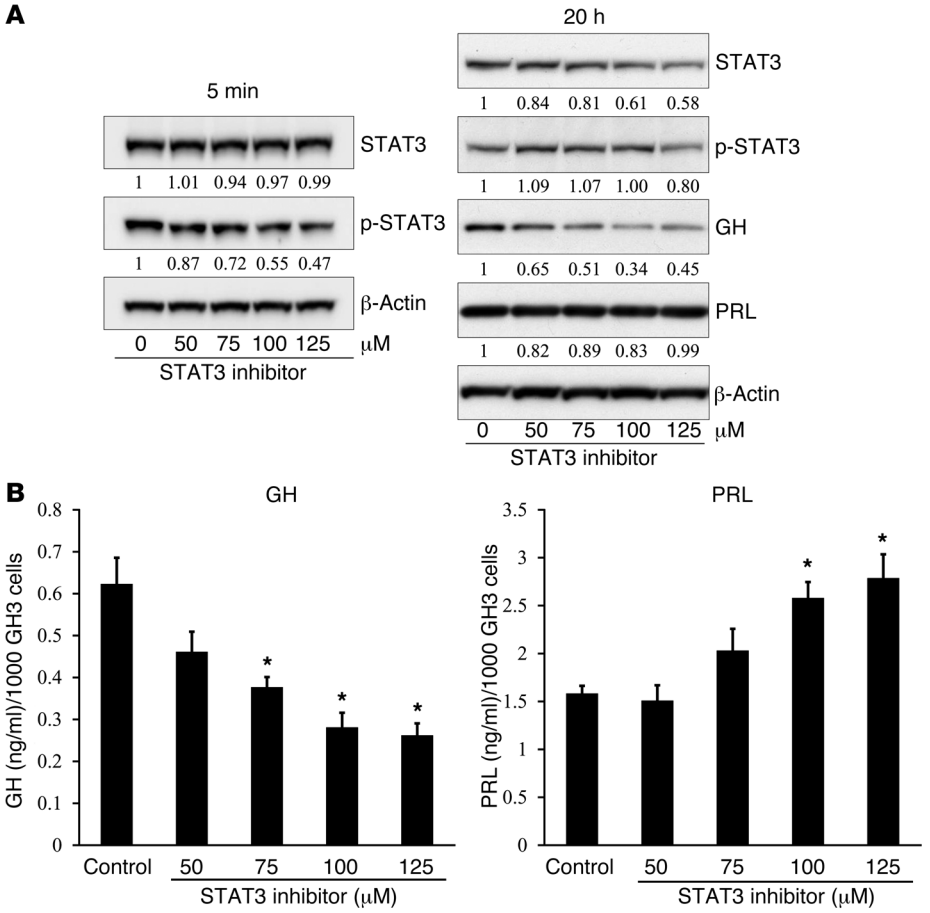

Figure 4. STAT3 inhibitor S3I-201 attenuates GH expression and secretion. (**A**) S3I-201 dose-dependently suppressed STAT3 phosphorylation and GH expression in GH3 cells, as measured by Western blot. Quantification of fold change, normalized with β-actin, is shown below each blot. (**B**) S3I-201 attenuated GH secretion in GH3 cells. Prolactin was measured to verify specific GH responses to S3I-201. Experiments were repeated 3 times. Representative experiments are shown. Results are presented as mean ± SEM. Student's *t* test, $^*P < 0.05$.

growth for the duration of the experiment (Figure 6B). Tumors derived from S3I-201–treated rats were significantly smaller than those from the untreated group (220 ± 16 mm^3 vs. 287 ± 16 mm^3; Student's *t* test, $P < 0.01$) as early as 5 days after S3I-201 injection. Fifteen days after treatments, the average tumor volume of S3I-201–treated rats was 64% of that of controls (449 ± 40 mm^3 vs. 708 ± 83 mm^3; Student's *t* test, $P < 0.01$). Rats were sacrificed and tumors were harvested 15 days after treatment initiation. The average tumor weight of S3I-201–treated rats was 78 ± 8 mg, while tumors derived from control rats weighed 114 ± 13 mg (32% reduction; Student's *t* test, $P < 0.05$). Animals appeared to tolerate S3I-201, showing no apparent signs of ill health and no differences in body weight. As measured by real-time PCR, intratumoral *Stat3* expression in the xenografts was significantly suppressed by S3I-201 treatment compared with that in vehicle controls (72% reduction; Student's *t* test, $P < 0.01$), and *Gh* expression also showed an approximately 30% reduction ($P = 0.08$, Student's *t* test) (Figure 6C). Blood samples collected 1 day before S3I-201 treatment (pretreatment as baseline) and 15 days after treatment (end point of treatment) were obtained in the morning (10–11 AM) to minimize GH fluctuations. As shown in Figure 6D, serum GH levels were attenuated in the S3I-201 treatment group as compared with those in controls (Student's *t* test, $P < 0.05$), while serum IGF1 levels decreased slightly.

STAT3 inhibitor S3I-201 attenuates GH in human somatotroph adenomas. Since the STAT3 inhibitor suppresses GH in rodent GH3 cells and in somatotrophic xenografts, we cultured primary cells derived from 21 human somatotroph adenomas after transsphenoidal resection (Supplemental Table 1), treated them with S3I-201 (0–150 μM) for 48 hours, and assessed *GH* gene expression and hormonal production. As assessed by real-time PCR using both *RPL13A* and *18S* as internal controls, *GH* mRNA levels were dose-dependently suppressed by S3I-201 by up to 64% in 17 of 21 (81%) tumor cell cultures (repeated-measures ANOVA, $P < 0.0001$), whereas 4 of 21 specimens did not respond (Figure 7A). Similar to mRNA expression, GH protein levels were dose-dependently inhibited by S3I-201 by up to 68% in 15 of 21 (71%) tumor cell cultures (repeated-measures ANOVA, $P < 0.0001$), as measured by Western blot (Figure 7B). Furthermore, media GH concentrations were markedly attenuated by S3I-201 by up to 60% in 13 of 21 (62%) tumor cell cultures (repeated-measures ANOVA, $P < 0.0001$), while in 8 samples, GH levels were unchanged (Figure 7C). Information for GH alterations in all 21 individual primary cultures is shown in Supplemental Figure 3. In primary cell cultures, β-actin and GAPDH were both affected by higher doses of S3I-201 (data not shown), and cell numbers could not be counted accurately. We therefore measured total protein in each group and used these results to normalize GH protein expression and secretion. Phosphorylated STAT3 at Tyr705 was also decreased in 17 primary cultures, as measured by Western blot, indicating efficient activity of S3I-201, while phospho-STAT3 was undetectable in 4 primary cultures due to the limited amount of protein extracted. Total STAT3 expression was also attenuated in most primary cultures. Detailed information regarding phospho-STAT3 and STAT3 responses is provided in Supplemental Figure 4. Figure 7D shows representative results of concordant GH reduction by S3I-201 in a primary human cell culture. These results confirmed the inhibitory effect of STAT3 inhibitor on human GH expression and secretion, suggesting STAT3 as a target for somatotroph adenoma therapy.

Discussion

Therapy for acromegaly caused by somatotroph pituitary adenomas is targeted at normalizing GH and IGF1 levels, decreasing mortality, and reducing tumor volume (29). Although transsphe-

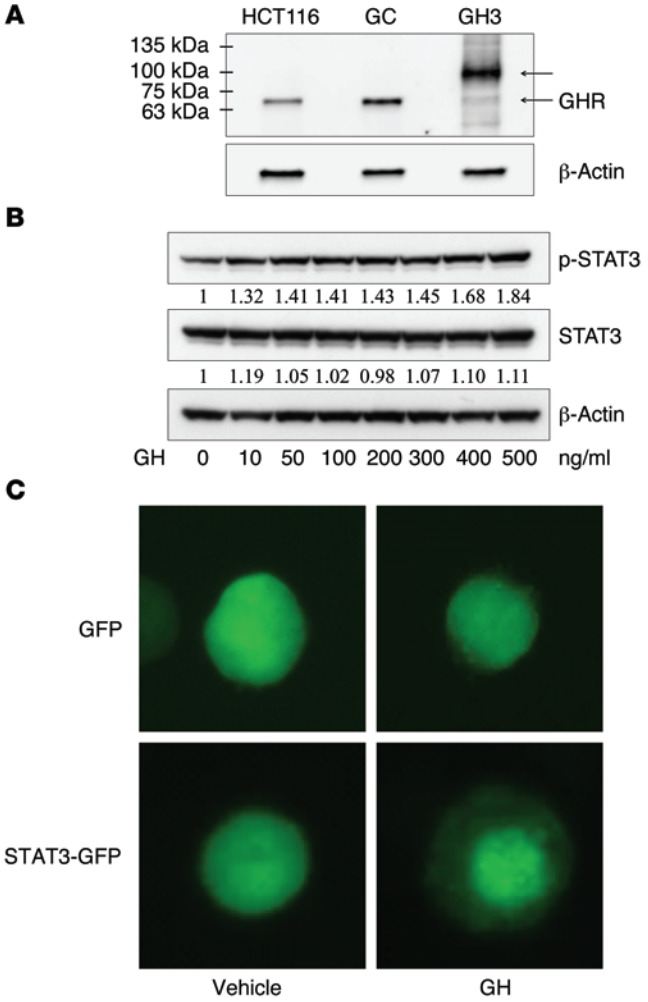

Figure 5. GH promotes STAT3 phosphorylation and nuclear translocation. (**A**) Detection of GHR expression in GH3 and GC cells, as measured by Western blot. (**B**) GH dose-dependently induced STAT3 phosphorylation in GH3 cells, as measured by Western blot. Quantification of fold change normalized with β-actin is shown below each blot. (**C**) GH promoted STAT3-GFP nuclear localization in GC cells. GC cells were transfected with pEGFP-N3 or STAT3/pEGFP-N3 plasmids, serum starved overnight, treated with vehicle or GH (500 ng/ml) for 6 hours, and imaged by fluorescent microscopy. Experiments were repeated 2 or 3 times, and figures show representative experiments. Original magnification, ×800.

noidal surgery is the primary treatment option for microadenomas (<10 mm) (30–32), invasive macroadenomas, which cannot be completely resected, are more prominent, and, as GH hypersecretion invariably persists postoperatively, surgical outcomes are poor (31). Somatostatin receptor ligands and the GHR antagonist are used for persistent or recurrent acromegaly following noncurative surgery and also as primary therapy for patients unsuitable for surgery (33). Identification of new therapeutic targets for acromegaly is important, as therapies are only maximally effective in approximately 50% of patients, while subsets of patients do not respond, and medications are associated with a variety of side effects (2, 3, 34–36).

Somatotroph tumorigenesis ensues as a consequence of unrestrained somatotroph proliferation associated with intrinsic cell-cycle dysfunction as well as altered regulation of both GH synthesis and secretion and somatotroph cell growth (2). In this study, we present evidence for a molecular mechanism that we believe to be novel, whereby STAT3 directly elicits GH production in somatotroph tumor cells. Although STAT3 is frequently activated in human cancers, expression in pituitary tumors has not been explored extensively. Downstream HGF/c-met effectors evaluated in pituitary adenomas showed positive STAT3 immunoreactivity in all adenomatous cell types (37). STAT3 was postulated to be involved in regulation of pituitary hormones, as two polymorphic *FGFR4* variants that correlate inversely with GH and PRL in rodent pituitary cells were associated with STAT3 phosphorylation (38). Here, we detected enhanced STAT3 expression in human somatotroph adenomas but not in nonsecreting pituitary tumor types, as previously shown for phospho-STAT3 (38), and also show selective concordant expression of STAT3 and GH in human somatotroph adenomas. STAT3 action is direct, as evidenced by its binding of the *Gh* promoter, induction of *Gh* transactivation and expression, and attenuation by STAT3-DN as well as the specific inhibitor S3I-201. As observed in fibroblasts (26), our results show that GH also induces somatotroph cell STAT3 phosphorylation and nuclear translocation. Based on these results, we postulate that GH participates in a positive autocrine or paracrine feedback for STAT3 induction, thus elucidating a novel mechanism for GH hypersecretion in somatotroph adenomas.

Persistent activation of STAT3 contributes to tumor growth and progression, and STAT3 has been identified as an attractive anticancer target (17, 39–41). The evidence for elevated somatotroph adenoma STAT3 and STAT3 regulation of GH suggests STAT3 as a potential cellular target to treat acromegaly. Small-molecule STAT3 inhibitors have been used in preclinical and clinical studies (17, 24, 25, 42–45), and we tested S3I-201, a cell-permeable amidosalicylic acid compound that selectively inhibits STAT3 DNA-binding activity in vitro (IC_{50} = 86 ± 33 μM) (24, 25). Here, we show that, using a dose of 5 mg/kg, S3I-201 inhibited rat GH3 pituitary cell growth in vitro and attenuated growth of somatotroph tumor xenografts in Wistar Furth rats. Tumor volumes, weight, and circulating GH were decreased. Furthermore, we verified inhibitory S3I-201 effects on *GH* mRNA, as assessed by real-time PCR in 17 of 21 of primary cell cultures derived from human somatotroph tumors, and on GH protein in 15 of 21 of cultures, as assessed by Western blotting. Medium GH concentrations were also suppressed in 13 of 21 cultures. *GH* mRNA expression of several cultures was attenuated, but medium GH levels did not respond to S3I-201, possibly indicating the need for longer treatment times or increased in vitro S3I-201 dose. Due to effects of high-dose S3I-201 on β-actin and GAPDH, and the impracticality of appropriate primary human cell counting, we used total protein harvested from each group to normalize GH protein expression and medium concentrations, thus normalization of medium GH levels was not maximally rigorous. Unfortunately, no hormonal secreting human pituitary cell line is available for study. STAT3 autoregulation has been reported in ectodermal cells (46, 47), and we show here that *Stat3* mRNA expression in somatotroph tumor xenografts was reduced by approximately 68% in S3I-201–treated tumors, verifying effective S3I-201 delivery to the xenografts via tail vein injection. Similarly, STAT3, as assessed by Western blot-

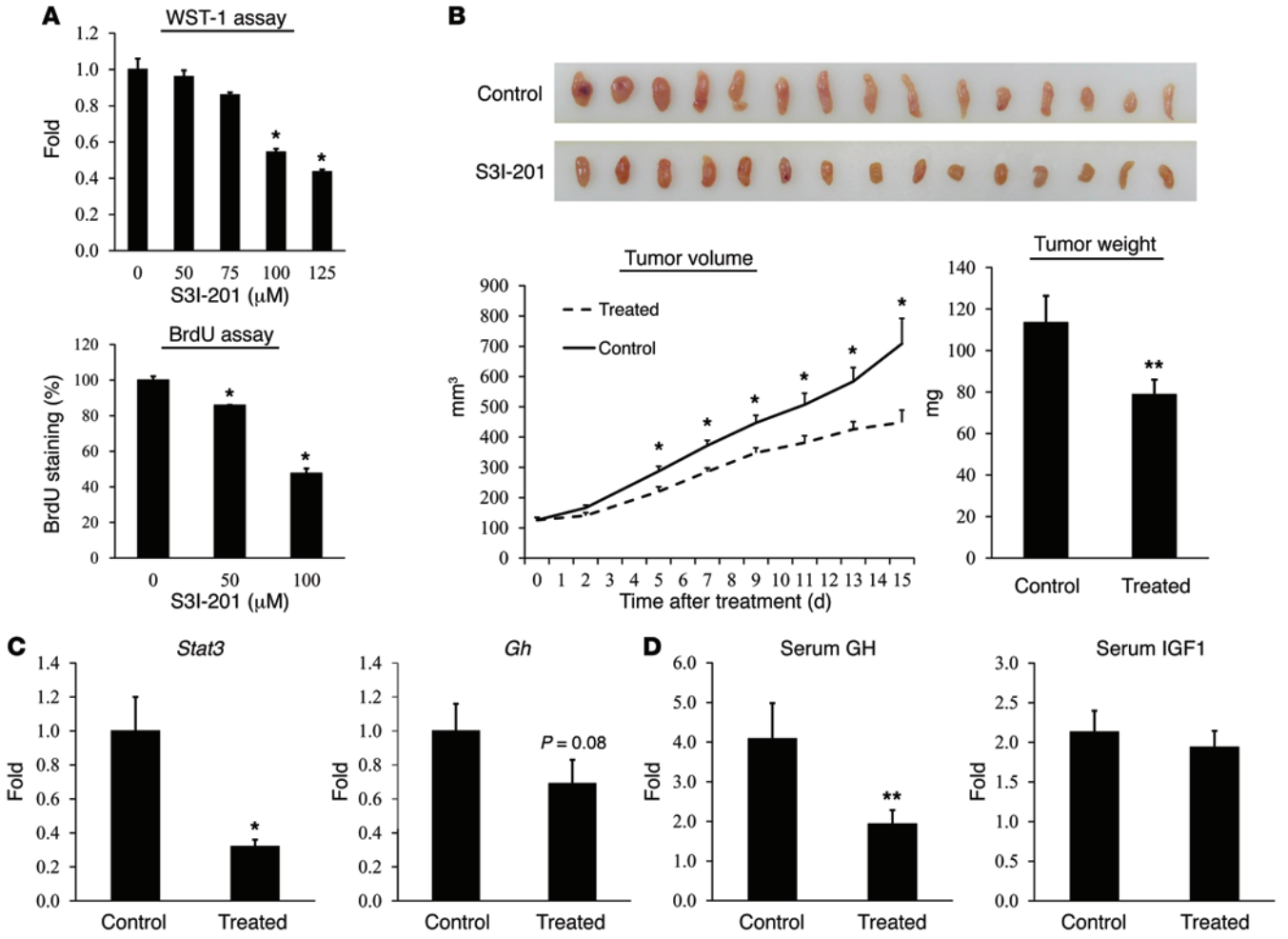

Figure 6. STAT3 inhibitor S3I-201 constrains somatotroph cell growth in vitro and somatotroph xenograft growth in vivo. (**A**) S3I-201 decreases GH3 cell growth in vitro. GH3 cells were treated with increasing amounts of S3I-201. Cell growth was measured by premixed WST-1 cell proliferation assay or BrdU incorporation. Experiments were repeated 2 or 3 times, and representative experiments are shown. (**B**) S3I-201 attenuated GH3 somatotroph xenograft growth in vivo. Thirty Wistar Furth rats were subcutaneously injected with GH3 cells. After 1 week, S3I-201 or vehicle (n = 15 per group) was injected intravenously at 5 mg/kg every 2 or 3 days for 2 weeks. Tumor size of the 30 rats was assessed twice a week, and tumor volume was calculated. Two weeks after treatment, animals were euthanized, and all 30 tumors were excised and weighed. (**C**) S3I-201 decreased xenograft *Gh* mRNA expression. Xenograft *Stat3* and *Gh* expression was assessed by real-time PCR, using *Gapdh* as a control. (**D**) S3I-201 decreased xenograft GH secretion. Blood samples were collected 1 day before treatment and on the day of euthanization. Serum GH and IGF1 levels were measured by RIA or ELISA, and fold change was calculated as serum level after treatment/serum level pretreatment. Results are presented as mean ± SEM, n = 15. Student's t test, $^*P < 0.01$, $^{**}P < 0.05$.

ting, was also reduced in most primary human cell cultures by higher S3I-201 doses. Taken together, we report in vivo, ex vivo, and in vitro evidence supporting the hypothesis that blocking STAT3 suppresses somatotroph tumor growth and inhibits GH hypersecretion. These results provide a rationale for using STAT3 inhibitors to treat benign GH-secreting pituitary tumors.

Methods

Tumor specimen immunofluorescence. Human pituitary tumor samples were obtained from the pathologist, and diagnosis of individual tumors was established on the basis of clinical features, histology, and pituitary hormone immunohistochemistry. We established a human somatotroph adenoma tissue array at the Yale Cancer Center/Pathology Tissue Microarray Facility (http://medicine.yale.edu/pathology/research/tissueservices), with samples obtained from verified pituitary tumor specimens. Slides were deparaffinized in xylene, hydrated in graded ethanol, and heated in Target Retrieval Solution (DakoCytomation) to retrieve antigen at 95°C for 40 minutes. Slides were permeabilized with 1% Triton X-100 in PBS for 30 minutes and incubated in blocking buffer (10% goat serum, 1% BSA, and 0.1% Triton X-100 in PBS). After washing, slides were hybridized with antibody against STAT3 (1:1,000; Cell Signaling catalog no. 9139) or against STAT3 and human GH (1:60,000; A.F. Parlow, Harbor-UCLA Research and Education Institute, Torrance, California, USA) at 4°C overnight. Alexa Fluor antibodies (Molecular Probes) were used as secondary antibodies and incubated at room temperature, avoiding light for 1 hour. Slides were mounted with ProLong Gold Antifade Reagent with DAPI (Life Technologies), and nuclei were dyed by DAPI with blue fluorescence.

Confocal microscopy. Samples were imaged with a Leica TCS/SP spectral confocal scanner (Leica Microsystems) in dual-emission mode to separate autofluorescence from specific staining. For single

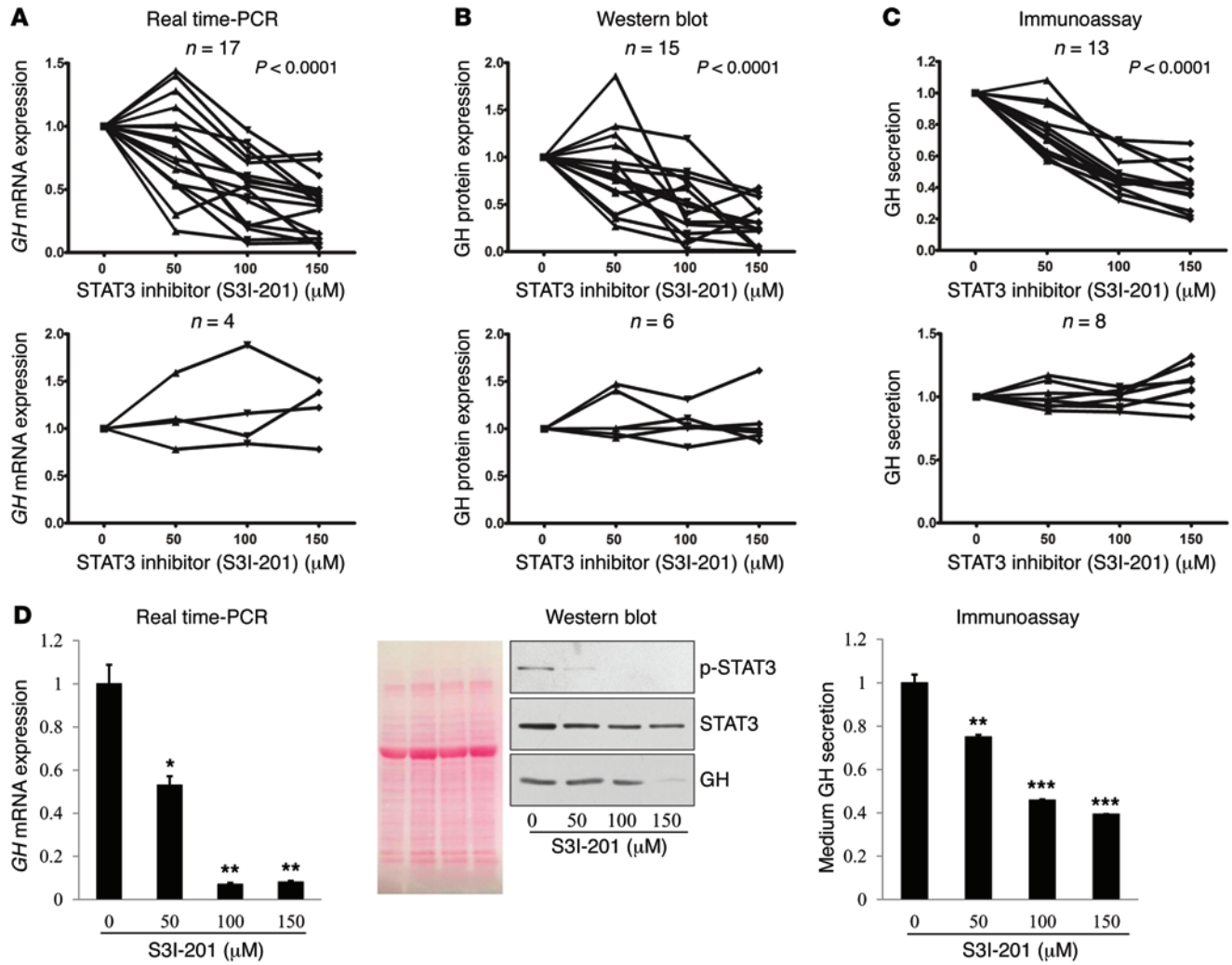

Figure 7. STAT3 inhibitor S3I-201 attenuates GH expression and secretion in primary cells derived from human somatotroph adenomas. (**A**) As assessed by real-time PCR, S3I-201 dose-dependently suppressed *GH* mRNA levels in 17 tumor cell cultures (repeated-measures ANOVA, $P < 0.0001$), whereas 4 specimens did not respond. (**B**) As measured by Western blot, S3I-201 dose-dependently inhibited GH protein levels in 15 tumor cell cultures (repeated-measures ANOVA, $P < 0.0001$), while GH was not altered in 6 tumor cell cultures. (**C**) As measured by immunoassay, S3I-201 dose-dependently attenuated medium GH secretion in 13 tumor cell cultures (repeated-measures ANOVA, $P < 0.0001$), while GH was unchanged in 8 tumor cell cultures. (**D**) Concordant *GH* mRNA and protein reductions by S3I-201 in a representative primary cell culture. The Ponceau staining blot indicates similar amounts of protein loading as that shown for Western blotting. Results are presented as mean ± SE. Student's *t* test, $^*P < 0.05$, $^{**}P < 0.01$, $^{***}P < 0.001$.

STAT3 staining, a spectral window of 500- to 550-nm wavelength detected Alexa Fluor 488 emission as green. A second window from 560 to 620 nm detected the autofluorescence contribution as red. As the 2 images were merged, autofluorescence appeared as yellow, and true signals appeared as green. For double staining, STAT3 stained with Alexa Fluor 488 was colored green, and GH stained with Alexa Fluor 568 was colored red and was imaged with a 540-nm HeNe laser.

Immunofluorescence evaluation. Immunofluorescent slides were examined independently by two blinded observers. Expression of STAT3 or GH was determined as a percentage of positively stained cells. For double staining, STAT3 expression was calculated as follows: +, if positively stained cells were <40% of total cells counted; ++, if stained cells were ≥40% and <60% of total cells counted; and +++, if stained cells were ≥60% of total cells counted. GH expression was evaluated as follows: +, if stained cells are <30% of total cells counted; ++, if stained cells are ≥30% and <50% of total cells counted; and +++, if stained cells are ≥50% of total cells counted. STAT3 and GH expression were correlated using Pearson χ^2 test with SPSS10.0 statistical software (IBM Software) and $P < 0.05$ considered significant.

Primary cell cultures derived from human somatotroph adenomas. Twenty-one somatotroph adenomas were obtained from patients with acromegaly at the time of surgical resection. Tumor tissues were transferred in 0.3% BSA–containing DMEM media. After washing, tumor tissues were chopped with a sterile scalpel into approximately 0.5- to 1-mm fragments, rinsed, and digested with DMEM containing 0.3% BSA, 0.35% collagenase, and 0.15% hyaluronidase at 37°C for 30 to 60 minutes (digestion time adjusted by tissue size). The mixture was centrifuged at 350 *g* for 5 minutes at 4°C, and the cell pellet was suspended in NeuroCult NS-A Basal Medium containing proliferation supplement (Stemcell Technologies) and antibiotics. Primary cells were aliquoted to 16 wells of 24-well plates precoated with ECL Cell Attachment Matrix (Millipore) and attached after 24-hour

incubation. Subsequently, culture medium was carefully removed, and medium containing S3I-201 was added at doses of 0 to 150 μM. After 48 hours, primary cells were harvested for total RNA and protein extraction by TRIzol (Life Technologies), and culture medium was collected. GH concentrations were normalized to total protein extracted from the same culture wells.

Cell culture, transfection and stable cell selection, and lentiviral infection. GH3 and GC cells were obtained from ATCC. GH3 cells were cultured in DMEM/F12 medium containing 15% horse serum, 2.5% fetal bovine serum, and Antibiotic-Antimycotic (Life Technologies). GC cells were cultured in DMEM medium containing 10% fetal bovine serum and Antibiotic-Antimycotic. Cell transfection was performed in wells with 70% to 80% confluent cells using Lipofectamine 2000 (Life Technologies). Geneticin (50 μg/ml) was added to GH3 transfectants for 14 days to select stable cells, which expressed ZsGreen. A mass population of green stable transfectants was sorted by the MoFlo Cell Sorter (Beckman Coulter) to ensure expression prior to performing experiments. Lentiviral infection was performed in 6-well plate with 70% to 80% confluent cells according to the Santa Cruz Biotechnology protocol. Cells were harvested 6 days later, and protein was extracted.

ChIP. Ten million GH3 cells were cross-linked and lysed using the ChIP-IT Express Kit (Active Motif). Chromatin was sonicated to 200- to 800-bp length fragments with 8 rounds of 10-second pulses using 25% power. Normalized, sheared chromatin DNA inputs were incubated with 4 μg negative control IgG or STAT3 antibody (Cell Signaling catalog no. 9139) overnight at 4°C. PCR reactions were amplified using precipitated immunocomplexes as templates and the following rat *Gh* promoter primers: primer 1 forward, 5′ CCACGCCCTGACTTAC 3′; primer 1 reverse, 5′ CTTAGAGGCTGCCAACT 3′; primer 2 forward, 5′ CATCAGTTTATGCTGCTATG 3′; primer 2 reverse, 5′ CTCCTCCTCCTGCTCTT 3′; primer 3 forward, 5′ GGCGGTGGAAAGGT 3′; primer 3 reverse, 5′ GGCGGAAGTTGGGAT 3′. Primer pairs were designed for different promoter regions, with primer 1 the furthest from ATG and primer 3 the closest to ATG.

Plasmids. Wild-type STAT3, STAT3-C, and STAT3-DN plasmids were cloned into pIRES2-ZsGreen1 vector (Clontech) (48). Wild-type STAT3 cDNA devoid of stop codons was cloned in frame to pEGFP-N3 vector (Clontech), which encodes the fusion STAT3-GFP protein. STAT3-DN was subcloned to the lenti-GFP vector and packaged, and viral particles were provided by the Viral Vector Core at Cedars-Sinai Medical Center. Lentiviral particles of rat *Stat3* shRNA and controls were purchased from Santa Cruz Biotechnology (catalog no. sc-270027-V and sc-108080). Rat *Gh* promoter –4,192/+167 was synthesized by GenScript and subcloned into $pGL_{4.10}$ vector (Promega) by Sac I and Nhe I. The shorter *Gh* promoter (–1,752/+167) in $pGL_{4.10}$ was modified from the –4,192/+167 promoter. The –4,192/+167 promoter was digested with Nhe I and EcoR I (internally located at –1,752/–1746 in the *Gh* promoter), blunted, and ligated.

Reporter assay. Stable GH3 STAT3/pIRES2-ZsGreen1 transfectants or pIRES2-ZsGreen1 controls were split into 24-well plates (5×10^5 cells per well) and separately transfected with rat *Gh* promoter –4,192/+167, promoter –1,752/+167, or $pGL_{4.10}$ luciferase vector as control (1.2 μg per well). Forty-eight hours later, whole-cell lysate was collected for reporter detection by the Dual Luciferase Reporter System (Promega). For STAT3 inhibitor S3I-201 (EMD Millipore) treatments, GH3 cells were transfected with 1 μg $pGL_{4.10}$ or rat *Gh* promoters (–4,192/+167 or –1,752/+167). Twenty-four hours later, cells were treated with STAT3 inhibitor (0–150 μM) for 24 hours, and protein was harvested for reporter assays. $pGL_{4.74}$ (hRluc/TK) encoding Renilla luciferase (Promega) was cotransfected as an internal control (10 ng per well) to assess transfection efficiency. Reactions were measured using an Orion Microplate Luminometer (Berthold Detection System). Transfections were performed in triplicate and repeated 3 times to assure reproducibility.

RNA extraction and real-time PCR. Total RNA were isolated by the RNeasy Mini Kit (QIAGEN). One microgram total RNA was used to synthesize cDNA with the iScript cDNA Synthesis Kit (Bio-Rad). For primary human cells derived from somatotroph adenomas, total RNA was extracted by TRIzol (Life Technologies) and 0.5 μg RNA was used for reverse transcription. Real-time PCR was amplified in 20 μl reaction mixtures (100 ng template, 0.5 μM of each primer, 10 μl 2× SYBR GREEN Master Mix [Life Technologies]) using the following parameters: 95°C for 1 minute, followed by 40 cycles of 95°C for 20 seconds, and 60°C for 40 seconds. *Gapdh* was used as an internal control. Rat *Stat3* (PPR44745B), *Gh* (PPR61690A), *Prl* (PPR06703A), and *Gapdh* (PPR06557A) primers as well as human *GH* (PPH00577B), *STAT3* (PPH00708F), and *18S* (PPH05666E) primers were all purchased from QIAGEN. Human *RPL13A* primers were designed as follows: forward, 5′-CCTGGAGGAGAAGAGGAAAGAGA-3′; reverse, 5′-TTGAGGACCTCTGTGTATTTGTCAA-3′.

Western blotting. Total cell lysate was prepared in RIPA buffer (Sigma-Aldrich) containing Protease Inhibitor Cocktail (Sigma-Aldrich). Total primary cell culture protein derived from human somatotroph tumors was isolated by TRIzol (Life Technologies). Protein concentrations were measured by the Coomassie Plus Assay Kit (Pierce) using BSA as standard. Equal amounts were separated by NuPAGE Novex Bis-Tris Gels (Life Technologies), transferred onto polyvinylidene difluoride membrane (Millipore), and incubated in blocking solution (TBS buffer containing 5% nonfat dry milk [Bio-Rad]) for 1 hour at room temperature, followed by incubation with primary antibody (STAT3: 1:1,000, Cell Signaling catalog no. 9139; phospho-STAT3 [Tyr705]: 1:500, Cell Signaling catalog no. 9131; STAT1: 1:1,000, Cell Signaling catalog no. 9172; phospho-STAT1 [Tyr701]: 1:500, Cell Signaling catalog no. 7649; STAT5: 1:1,000, Cell Signaling catalog no. 9358; phospho-STAT5 [Tyr694]: 1:500, Cell Signaling catalog no. 4322; rat GH and PRL antibodies, 1:2,000, A.F. Parlow, Harbor-UCLA Research and Education Institute; human GH: 1:5,000, R&D Systems AF1067; actin: 1:10,000, Millipore catalog no. MAB1501) at 4°C overnight. After 0.5% Tween-20 in TBS washings, membranes were incubated with horseradish peroxidase–linked secondary antibody (GE Healthcare) for 1 hour at room temperature and developed using ECL Western Blotting Detection Reagents (GE Healthcare). Western blots were quantified by ImageJ (NIH).

Hormone radioimmunoassay and ELISA. Rat GH radioimmunoassay (RIA) was performed in triplicate, using reagents provided by A.F. Parlow at the National Hormone and Peptide Program (Harbor-UCLA Medical Center). Iodination of rat GH (5 μg) with iodine-125 (500 μCi; Perkin-Elmer Life & Analytical Sciences) mixed with 0.1 mg Iodo-Gen (Pierce) was performed using 10 ml G-75 Sephadex columns (Sigma-Aldrich). Rat serum prolactin and IGF1 concentrations were measured by ELISA (prolactin, MD Biosciences; IGF1, ALIPCO). Human GH was measured by IMMULITE 2000 Immunoassay System (Siemens).

Cell proliferation assay. For WST-1 cell proliferation assays, GH3 cells (5×10^3 cells) were plated in flat-bottomed 96-well plates in 100 μl culture medium and treated with vehicle or S3I-201 at 50 to 125 μM. Each group consisted of 6 parallel wells. After 72 hours, premixed WST-1 cell proliferation reagent (Clontech) was added (1:10) and incubated for 4 hours at 37°C in a humidified atmosphere maintained at 5% CO_2, after which absorbance was measured at 450 nm.

For BrdU incorporation, GH3 cells (1×10^6 cells) were plated in 60-mm plates in 20 ml culture medium and treated with vehicle or S3I-201 at 50 to 100 μM. Each group consisted of 3 parallel plates. After 48 hours, BrdU was added to the culture medium at 1:1,000 and incubated for 40 minutes at 37°C in a humidified atmosphere maintained at 5% CO_2. Cells were stained for BrdU (5-Bromo-2′-deoxy-uridine Labeling and Detection Kit II, Roche) and counted by FACS.

Xenograft transplantation and in vivo tumor studies. Four-week-old female Wistar Furth rats were purchased from Harlan, and animal protocols were approved by the Cedars-Sinai Institutional Animal Care and Use Committee. GH3 cells (5×10^5 cells in 100 μl Matrigel) were subcutaneously injected into the left lumbar area. After 7 days, tumors with a volume of approximately 100 mm^3 were established. Rats were given S3I-201 intravenously at 5 mg/kg every 2 or 3 days for 2 weeks. Tumor size was measured by caliper measurements twice a week, and volume was calculated as follows: volume = (length × $width^2$)/2. Three weeks after cell inoculations, animals were euthanized and excised tumors were weighed. Blood samples were collected 1 day before S3I-201 treatment and again on the day of euthanization. Serum GH and prolactin were assessed by RIA or ELISA, respectively.

Statistics. For STAT3 immunofluorescence in human pituitary tumors (Figure 1B), groups were compared by 2-tailed unpaired *t* test. For STAT3 and GH costaining (Figure 1C), correlation was analyzed by Pearson χ^2 test. For GH expression in primary human pituitary cultures (Figure 7, A–C), groups were compared by repeated-measures ANOVA. All other comparisons were analyzed by 2-tailed Student's *t* test. *P* values of less than 0.05 were considered statistically significant.

Study approval. The protocol for collecting human pituitary specimens for immunofluorescence was approved by the Cedars-Sinai Medical Center Institutional Review Board, and informed consent was obtained. The protocol for harvesting human pituitary specimens for primary cultures was approved by the Peking Union Medical College Hospital Institutional Review Board, and informed consent was obtained. Animal protocols were approved by the Cedars-Sinai Institutional Animal Care and Use Committee.

Acknowledgments

We thank Bowen Sun and Yakun Yang (Department of Neurosurgery of Peking Union Medical College Hospital); Ningzhi Xu (Cancer Institute of Chinese Academy of Medical Sciences); Roy Heltsley and Svetlana Zonis for technical assistance; Serguei Bannykh (Department of Pathology, Cedars-Sinai Medical Center) for provision of human slide specimens; Patricia Lin (the Flow Cytometry Core of Cedars-Sinai Medical Center) and Vaithi Arumugaswami (the Viral Vector Core of Cedars-Sinai Medical Center); and A.F. Parlow (National Hormone and Peptide Program, Harbor-UCLA Medical Center) for providing GH and PRL antibodies. This work was supported by NIH grants CA75979 and DK 103198 (to S. Melmed), the Pfizer ASPIRE Young Investigator Research Award WI196457 (to C. Zhou), and the Doris Factor Molecular Endocrinology Laboratory.

Address correspondence to: Shlomo Melmed, Cedars-Sinai Medical Center, Room 2015, Los Angeles, California 90048, USA. Phone: 310.423.4691; E-mail: Melmed@csmc.edu.

1. Jagannathan J, et al. Genetics of pituitary adenomas: current theories and future implications. *Neurosurg Focus*. 2005;19(5):E4.
2. Melmed S. Acromegaly pathogenesis and treatment. *J Clin Invest*. 2009;119(11):3189–3202.
3. Melmed S. Medical progress: acromegaly. *N Engl J Med*. 2006;355(24):2558–2573.
4. Kopchick JJ, Parkinson C, Stevens EC, Trainer PJ. Growth hormone receptor antagonists: discovery, development, and use in patients with acromegaly. *Endocr Rev*. 2002;23(5):623–646.
5. Giustina A, Veldhuis JD. Pathophysiology of the neuroregulation of growth hormone secretion in experimental animals and the human. *Endocr Rev*. 1998;19(6):717–797.
6. Casanueva FF, Camina JP, Carreira MC, Pazos Y, Varga JL, Schally AV. Growth hormone-releasing hormone as an agonist of the ghrelin receptor GHS-R1a. *Proc Natl Acad Sci U S A*. 2008;105(51):20452–20457.
7. Zhu X, Lin CR, Prefontaine GG, Tollkuhn J, Rosenfeld MG. Genetic control of pituitary development and hypopituitarism. *Curr Opin Genet Dev*. 2005;15(3):332–340.
8. Melmed S. Pathogenesis of pituitary tumors. *Nat Rev Endocrinol*. 2011;7(5):257–266.
9. Darnell JE Jr, Kerr IM, Stark GR. Jak-STAT pathways and transcriptional activation in response to IFNs and other extracellular signaling proteins. *Science*. 1994;264(5164):1415–1421.
10. Darnell JE Jr. STATs and gene regulation. *Science*. 1997;277(5332):1630–1635.
11. Buettner R, Mora LB, Jove R. Activated STAT signaling in human tumors provides novel molecular targets for therapeutic intervention. *Clin Cancer Res*. 2002;8(4):945–954.
12. Aggarwal BB, et al. Signal transducer and activator of transcription-3, inflammation, and cancer: how intimate is the relationship? *Ann N Y Acad Sci*. 2009;1171:59–76.
13. Bromberg J. Stat proteins and oncogenesis. *J Clin Invest*. 2002;109(9):1139–1142.
14. Turkson J, et al. Phosphotyrosyl peptides block Stat3-mediated DNA binding activity, gene regulation, and cell transformation. *J Biol Chem*. 2001;276(48):45443–45455.
15. Siddiquee K, et al. Selective chemical probe inhibitor of Stat3, identified through structure-based virtual screening, induces antitumor activity. *Proc Natl Acad Sci U S A*. 2007;104(18):7391–7396.
16. Yue P, Turkson J. Targeting STAT3 in cancer: how successful are we? *Expert Opin Investig Drugs*. 2009;18(1):45–56.
17. Wang X, Crowe PJ, Goldstein D, Yang JL. STAT3 inhibition, a novel approach to enhancing targeted therapy in human cancers (review). *Int J Oncol*. 2012;41(4):1181–1191.
18. Arzt E. gp130 cytokine signaling in the pituitary gland: a paradigm for cytokine-neuro-endocrine pathways. *J Clin Invest*. 2001;108(12):1729–1733.
19. Stefana B, Ray DW, Melmed S. Leukemia inhibitory factor induces differentiation of pituitary corticotroph function: an immuno-neuroendocrine phenotypic switch. *Proc Natl Acad Sci U S A*. 1996;93(22):12502–12506.
20. Ray DW, Ren SG, Melmed S. Leukemia inhibitory factor (LIF) stimulates proopiomelanocortin (POMC) expression in a corticotroph cell line. Role of STAT pathway. *J Clin Invest*. 1996;97(8):1852–1859.
21. Bousquet C, Melmed S. Critical role for STAT3 in murine pituitary adrenocorticotropin hormone leukemia inhibitory factor signaling. *J Biol Chem*. 1999;274(16):10723–10730.
22. Bousquet C, Zatelli MC, Melmed S. Direct regulation of pituitary proopiomelanocortin by STAT3 provides a novel mechanism for immuno-neuroendocrine interfacing. *J Clin Invest*. 2000;106(11):1417–1425.
23. Mynard V, Guignat L, Devin-Leclerc J, Bertagna X, Catelli MG. Different mechanisms for leukemia inhibitory factor-dependent activation of two proopiomelanocortin promoter regions. *Endocrinology*. 2002;143(10):3916–3924.
24. Siddiquee K, et al. Selective chemical probe inhibitor of Stat3, identified through struc-

ture-based virtual screening, induces antitumor activity. *Proc Natl Acad Sci U S A*. 2007;104(18):7391–7396.
25. Lin L, et al. The STAT3 inhibitor NSC 74859 is effective in hepatocellular cancers with disrupted TGF-β signaling. *Oncogene*. 2009;28(7):961–972.
26. Campbell GS, Meyer DJ, Raz R, Levy DE, Schwartz J, Carter-Su C. Activation of acute phase response factor (APRF)/Stat3 transcription factor by growth hormone. *J Biol Chem*. 1995;270(8):3974–3979.
27. Herrington J, Smit LS, Schwartz J, Carter-Su C. The role of STAT proteins in growth hormone signaling. *Oncogene*. 2000;19(21):2585–2597.
28. Sustarsic EG, Junnila RK, Kopchick JJ. Human metastatic melanoma cell lines express high levels of growth hormone receptor and respond to GH treatment. *Biochem Biophys Res Commun*. 2013;441(1):144–150.
29. Giustina A, et al. Expert consensus document: A consensus on the medical treatment of acromegaly. *Nat Rev Endocrinol*. 2014;10(4):243–248.
30. Kreutzer J, Vance ML, Lopes MB, Laws ER Jr. Surgical management of GH-secreting pituitary adenomas: an outcome study using modern remission criteria. *J Clin Endocrinol Metab*. 2001;86(9):4072–4077.
31. Shimon I, Cohen ZR, Ram Z, Hadani M. Transsphenoidal surgery for acromegaly: endocrinological follow-up of 98 patients. *Neurosurgery*. 2001;48(6):1239–1243.
32. Starke RM, et al. Endoscopic vs microsurgical transsphenoidal surgery for acromegaly: outcomes in a concurrent series of patients using modern criteria for remission. *J Clin Endocrinol Metab*. 2013;98(8):3190–3198.
33. Burt MG, Ho KK. Comparison of efficacy and tolerability of somatostatin analogs and other therapies for acromegaly. *Endocrine*. 2003;20(3):299–305.
34. Giustina A, Porcelli T. Pituitary gland: medical therapy for acromegaly: can we predict response? *Nat Rev Endocrinol*. 2009;5(8):425–427.
35. Sherlock M, Woods C, Sheppard MC. Medical therapy in acromegaly. *Nat Rev Endocrinol*. 2011;7(5):291–300.
36. Colao A, et al. Pasireotide versus octreotide in acromegaly: a head-to-head superiority study. *J Clin Endocrinol Metab*. 2014;99(3):791–799.
37. Trovato M, et al. HGF/c-met system targeting PI3K/AKT and STAT3/phosphorylated-STAT3 pathways in pituitary adenomas: an immunohistochemical characterization in view of targeted therapies. *Endocrine*. 2013;44(3):735–743.
38. Tateno T, Asa SL, Zheng L, Mayr T, Ullrich A, Ezzat S. The FGFR4-G388R polymorphism promotes mitochondrial STAT3 serine phosphorylation to facilitate pituitary growth hormone cell tumorigenesis. *PLoS Genet*. 2011;7(12):e1002400.
39. Sen M, et al. Targeting Stat3 abrogates EGFR inhibitor resistance in cancer. *Clin Cancer Res*. 2012;18(18):4986–4996.
40. Masciocchi D, Gelain A, Villa S, Meneghetti F, Barlocco D. Signal transducer and activator of transcription 3 (STAT3): a promising target for anticancer therapy. *Future Med Chem*. 2011;3(5):567–597.
41. Huang S. Regulation of metastases by signal transducer and activator of transcription 3 signaling pathway: clinical implications. *Clin Cancer Res*. 2007;13(5):1362–1366.
42. Song H, Wang R, Wang S, Lin J. A low-molecular-weight compound discovered through virtual database screening inhibits Stat3 function in breast cancer cells. *Proc Natl Acad Sci U S A*. 2005;102(13):4700–4705.
43. Zhang X, Yue P, Fletcher S, Zhao W, Gunning PT, Turkson J. A novel small-molecule disrupts Stat3 SH2 domain-phosphotyrosine interactions and Stat3-dependent tumor processes. *Biochem Pharmacol*. 2010;79(10):1398–1409.
44. Siddiquee KA, et al. An oxazole-based small-molecule Stat3 inhibitor modulates Stat3 stability and processing and induces antitumor cell effects. *ACS Chem Biol*. 2007;2(12):787–798.
45. Lin L, et al. A novel small molecule, LLL12, inhibits STAT3 phosphorylation and activities and exhibits potent growth-suppressive activity in human cancer cells. *Neoplasia*. 2010;12(1):39–50.
46. Nichane M, Ren X, Bellefroid EJ. Self-regulation of Stat3 activity coordinates cell-cycle progression and neural crest specification. *EMBO J*. 2010;29(1):55–67.
47. Hutchins AP, et al. Distinct transcriptional regulatory modules underlie STAT3's cell type-independent and cell type-specific functions. *Nucleic Acids Res*. 2013;41(4):2155–2170.
48. Zhou C, Tong Y, Wawrowsky K, Melmed S. PTTG acts as a STAT3 target gene for colorectal cancer cell growth and motility. *Oncogene*. 2014;33(7):851–861.